Compressed Channel Estimation and Joint Beamforming for Intelligent Reflecting Surface-Assisted Millimeter Wave Systems

Peilan Wang, Jun Fang, Huiping Duan, and Hongbin Li, *Fellow, IEEE*

arXiv:1911.07202v2 [eess.SP] 20 Nov 2019

***Abstract*— In this paper, we consider channel estimation and joint beamforming design for Intelligent reflecting surface (IRS)-assisted millimeter wave (mmWave) multiple-input single-output (MISO) systems, where an IRS is deployed to assist the data transmission from the base station (BS) to a single-antenna user. To reduce the training overhead, sparsity inherent in mmWave channels is exploited. We first find a sparse representation of the cascade channel, and then develop a compressed sensing-based channel estimation method. Joint beamforming design is discussed based on the estimated channel. Simulation results show that our proposed method is able to provide an accurate channel estimation, meanwhile achieving a substantial training overhead reduction.**

***Index Terms*— Intelligent reflecting surface, millimeter wave communications, channel estimation.**

I. Introduction

Intelligent reflecting surface (IRS) comprising a large number of passive reflecting elements is emerging as a promising technology for realizing a smart and programmable wireless propagation environment via software-controlled reflection [1], [2]. With a smart controller, each element can independently reflect the incident signal with a reconfigurable amplitude and phase shift. By properly adjusting the phase shifts of the passive elements, the reflected signals can add coherently at the desired receiver to improve the signal power. Recently, IRS has been introduced to establish robust mmWave connections even when the line-of-sight (LOS) link is blocked by obstructions [3], [4]. To reach the full potential of IRSs, accurate channel state information (CSI) is required for joint active and passive beamforming. Nevertheless, channel estimation for IRS-assisted systems faces multiple challenges. First, due to the large number of passive reflecting elements used by the IRS, the channel matrix to be estimated has a large size, which makes it difficult to acquire accurate CSI during a practical channel coherence time. Second, IRS consisting of passive elements can only reflect the incoming signals, which means that only the concatenated (cascade) channel can be sensed at the receiver.

There are already some works on channel estimation for IRS-aided wireless systems, e.g. [5]–[9]. In [5], to facilitate channel estimation, active elements were used at the IRS. Besides the passive reflecting mode, active elements can also operate in a receive mode so that they can receive incident signals to help estimate the BS-IRS channel and the IRS-user channel. IRSs with active elements, however, need wiring or battery power, which may not be feasible for many applications. For IRSs with all passive elements, estimating the cascade BS-IRS-user channel suffices for joint beamforming. In [6], [7], least square (LS) estimation methods were proposed to estimate uplink cascade channels. The problem lies in that the cascade channel usually has a large size. These methods which do not exploit the sparse structure inherent in wireless channels may incur a considerable amount of training overhead. In [8], a sparse matrix factorization-based channel estimation method was developed by exploiting the low-rank structure of the BS-IRS and IRS-user channels. To induce sparsity, this method requires to switch off some randomly selected passive elements at each time. Implementing the ON/OFF switching, however, is costly as this requires separate amplitude control of each IRS element [9].

In this paper, we consider the problem of channel estimation for IRS-assisted mmWave MISO systems. To reduce the training overhead, sparsity inherent in mmWave channels is exploited. By exploiting properties of the Khatri-Rao and Kronecker products, we first find a sparse representation of the concatenated BS-IRS-user (cascade) channel. We then develop a compressed sensing method for channel estimation. Unlike [6], [8], our proposed method does not need to switch off passive elements, thus avoiding separate amplitude control of each IRS element. Simulation results show that our proposed method, with only a small amount of training overhead, can provide reliable channel estimation and help attain a decent beamforming gain.

II. System Model and Problem Formulation

We consider an IRS-assisted mmWave downlink system, where an IRS is deployed to assist the data transmission from the BS to a single-antenna user. Suppose the IRS is a planar array with M reflecting elements. The BS is equipped with N antennas. Let $\boldsymbol{G} \in \mathbb{C}^{M\times N}$ denote the channel from the BS to the IRS, and $\boldsymbol{h}_r \in \mathbb{C}^M$ denote the channel from the IRS to the

Peilan Wang, and Jun Fang are with the National Key Laboratory of Science and Technology on Communications, University of Electronic Science and Technology of China, Chengdu 611731, China, Email: peilan_wangle@std.uestc.edu.cn, JunFang@uestc.edu.cn

Huiping Duan is with the School of Information and Communications Engineering, University of Electronic Science and Technology of China, Chengdu 611731, China, Email: huipingduan@uestc.edu.cn

Hongbin Li is with the Department of Electrical and Computer Engineering, Stevens Institute of Technology, Hoboken, NJ 07030, USA, E-mail: Hongbin.Li@stevens.edu

This work was supported in part by the National Science Foundation of China under Grant 61829103 and Grant 61871091.

user. To better illustrate our idea, we neglect the direct link from the BS to the user. In practice, the direct link may not be available due to unfavorable propagation conditions. Also, even if the direct link between the BS and the user exists, it can be estimated by turning off the IRS and then canceled from the model [8]. Each reflecting element of the IRS can reflect the incident signal with a reconfigurable phase shift and amplitude via a smart controller [1]. Denote

$$\boldsymbol{\Theta} \triangleq \text{diag}(\beta_1 e^{j\theta_1}, \ldots, \beta_M e^{j\theta_M}) \tag{1}$$

as the phase-shift matrix of the IRS, where $\theta_m \in [0, 2\pi]$ and $\beta_m \in [0, 1]$ denote the phase shift and amplitude reflection coefficient associated with the mth passive element of the IRS, respectively. For simplicity, we assume $\beta_m = 1, \forall m$ in the sequel of this paper.

Let $\boldsymbol{w} \in \mathbb{C}^N$ denote the beamforming vector adopt by the BS. The signal received by the user at the tth time instant is given by

$$\begin{aligned} y(t) &= \boldsymbol{h}_r^H \boldsymbol{\Theta}(t) \boldsymbol{G} \boldsymbol{w}(t) s(t) + \epsilon(t) \\ &\overset{(a)}{=} \boldsymbol{v}^H(t) \text{diag}(\boldsymbol{h}_r^H) \boldsymbol{G} \boldsymbol{w}(t) s(t) + \epsilon(t) \\ &\overset{(b)}{=} \boldsymbol{v}^H(t) \boldsymbol{H} \boldsymbol{w}(t) s(t) + \epsilon(t) \end{aligned} \tag{2}$$

where $s(t)$ is the transmitted symbol, $\epsilon(t)$ denotes the additive white Gaussian noise with zero mean and variance σ^2, in (a), we define $\boldsymbol{v} \triangleq [e^{j\theta_1} \ \ldots \ e^{j\theta_M}]^H$, and in (b), we define $\boldsymbol{H} \triangleq \text{diag}(\boldsymbol{h}_r^H)\boldsymbol{G}$. Here $\boldsymbol{H}$ is referred to as the cascade channel. An important observation based on (2) is that we only need the knowledge of the cascade channel $\boldsymbol{H}$ for joint active and passive beamforming. Therefore our objective is to estimate the cascade channel $\boldsymbol{H}$ from the received measurements $\{y(t)\}_{t=1}^T$. Note that to facilitate channel estimation, different precoding vectors and phase shift matrices are employed for different time instants. In addition, although a downlink scenario is considered in this paper, our proposed method can be easily adapted to solve the uplink channel estimation problem.

The cascade channel matrix $\boldsymbol{H}$ has a dimension of $M \times N$. Both N and M could be large for mmWave systems. As a result, the number of channel parameters to be estimated is very large, which makes channel estimation a challenging problem. On the other hand, extensive experimental measurements [10], [11] have shown that mmWave channels exhibit some inherent sparse scattering characteristics, which can be utilized to substantially reduce the training overhead. The crux here is to obtain a sparse representation of the cascade channel $\boldsymbol{H}$. Before we proceed to address this problem, let us first discuss the channel model for the BS-IRS channel $\boldsymbol{G}$ and the IRS-user channel $\boldsymbol{h}_r$.

III. Channel Model

A narrowband geometric channel model [12] is used to characterize the BS-IRS channel $\boldsymbol{G}$ and the IRS-user channel $\boldsymbol{h}_r$. Specifically, the BS-IRS channel can be modeled as

$$\boldsymbol{G} = \sum_{l=1}^{L} \varrho_l \boldsymbol{a}_r(\vartheta_l, \gamma_l) \boldsymbol{a}_t^H(\phi_l) \tag{3}$$

where L is the number of paths, ϱ_l denotes the complex gain associated with the lth path, ϑ_l (γ_l) denotes the azimuth (elevation) angle of arrival (AoA), ϕ_l is the angle of departure (AoD), $\boldsymbol{a}_r$ and $\boldsymbol{a}_t$ represent the receive and transmit array response vectors, respectively. Suppose the IRS is an $M_x \times M_y$ uniform planar array (UPA). We have

$$\boldsymbol{a}_r(\vartheta_l, \gamma_l) = \boldsymbol{a}_x(u) \otimes \boldsymbol{a}_y(v) \tag{4}$$

where $\otimes$ stands for the Kronecker product, $u \triangleq 2\pi d \cos(\gamma_l)/\lambda$, $v \triangleq 2\pi d \sin(\gamma_l)\cos(\vartheta_l)/\lambda$, d denotes the antenna spacing, λ is the signal wavelength, and

$$\begin{aligned} \boldsymbol{a}_x(u) &\triangleq [1 \ \ e^{ju} \ \ \ldots \ \ e^{j(M_x-1)u}]^T \\ \boldsymbol{a}_y(v) &\triangleq [1 \ \ e^{jv} \ \ \ldots \ \ e^{j(M_y-1)v}]^T \end{aligned} \tag{5}$$

Due to the sparse scattering nature of mmWave channels, the number of path L is small relative to the dimensions of $\boldsymbol{G}$. Hence we can express $\boldsymbol{G}$ as

$$\boldsymbol{G} = (\boldsymbol{F}_x \otimes \boldsymbol{F}_y)\boldsymbol{\Sigma}\boldsymbol{F}_L^H \triangleq \boldsymbol{F}_P \boldsymbol{\Sigma} \boldsymbol{F}_L^H \tag{6}$$

where $\boldsymbol{F}_L \in \mathbb{C}^{N \times N_G}$ is an overcomplete matrix ($N_G \geq N$) and each of its columns has a form of $\boldsymbol{a}_t(\phi_l)$, with ϕ_l chosen from a pre-discretized grid, $\boldsymbol{F}_x \in \mathbb{C}^{M_x \times M_{G,x}}$ ($\boldsymbol{F}_y \in \mathbb{C}^{M_y \times M_{G,y}}$) is similarly defined with each of its columns having a form of $\boldsymbol{a}_x(u)$ ($\boldsymbol{a}_y(v)$), and u (v) chosen from a pre-discretized grid [13], $\boldsymbol{\Sigma} \in \mathbb{C}^{M_G \times N_G}$ is a sparse matrix with L non-zero entries corresponding to the channel path gains $\{\varrho_l\}$, in which $M_G = M_{G,x} \times M_{G,y}$. Here for simplicity, we assume that the true AoA and AoD parameters lie on the discretized grid. In practice, the true parameters do not necessarily lie on the discretized grid, which is referred to as grid or basis mismatch. In the presence of grid mismatch, the number of nonzero entries in the beam space channel will not exactly equal to the number of paths. Instead, the number of nonzero entries will become larger due to the power leakage caused by grid mismatch.

The IRS-user channel can be modeled as

$$\boldsymbol{h}_r = \sum_{l=1}^{L'} \alpha_l \boldsymbol{a}_r(\vartheta_l, \gamma_l) \tag{7}$$

where α_l denotes the complex gain associated with the lth path, and ϑ_l (γ_l) denotes the azimuth (elevation) angle of departure. Due to limited scattering characteristics, the IRS-user channel can be written as

$$\boldsymbol{h}_r = \boldsymbol{F}_P \boldsymbol{\alpha} \tag{8}$$

where $\boldsymbol{\alpha} \in \mathbb{C}^{M_G}$ is a sparse vector with L' nonzero entries.

IV. Proposed Method

A. Channel Estimation

We now discuss how to develop a compressed sensing-based method to estimate the cascade channel $\boldsymbol{H}$. To formulate channel estimation into a sparse signal recovery problem, we need to utilize the sparsity inherent in the cascade channel $\boldsymbol{H}$. Although both $\boldsymbol{G}$ and $\boldsymbol{h}_r$ are sparse in the beam space domain, obtaining a sparse representation for their cascade form $\boldsymbol{H} = \text{diag}(\boldsymbol{h}_r^H)\boldsymbol{G}$ is not that straightforward and constitutes the main

contribution of our paper. Let $\bullet$ denote the "transposed Khatri-Rao product", we can express the cascade channel as

$$\begin{aligned}\boldsymbol{H} &= \text{diag}(\boldsymbol{h}_r^H)\boldsymbol{G} \\ &\overset{(a)}{=} \boldsymbol{h}_r^* \bullet \boldsymbol{G} \\ &\overset{(b)}{=} (\boldsymbol{F}_P^*\boldsymbol{\alpha}^*) \bullet (\boldsymbol{F}_P\boldsymbol{\Sigma}\boldsymbol{F}_L^H) \\ &\overset{(c)}{=} (\boldsymbol{F}_P^* \bullet \boldsymbol{F_P})(\boldsymbol{\alpha}^* \otimes (\boldsymbol{\Sigma}\boldsymbol{F}_L^H)) \\ &\overset{(d)}{=} (\boldsymbol{F}_P^* \bullet \boldsymbol{F}_P)(\boldsymbol{\alpha}^* \otimes \boldsymbol{\Sigma})(1 \otimes \boldsymbol{F}_L^H) \\ &\overset{(e)}{=} \boldsymbol{D}(\boldsymbol{\alpha}^* \otimes \boldsymbol{\Sigma})\boldsymbol{F}_L^H \end{aligned} \tag{9}$$

where $(\cdot)^*$ denotes the complex conjugate in (a), (b) comes from (6) and (8), (c) follows from the property of Khatri-Rao product and (d) is obtained by resorting to the property of Kronecker product, and we define

$$\boldsymbol{D} \triangleq \boldsymbol{F}_P^* \bullet \boldsymbol{F}_P \tag{10}$$

in (e). Since both $\boldsymbol{\alpha}$ and $\boldsymbol{\Sigma}$ are sparse, their Kronecker product is also sparse. We see that after a series of transformation, a sparse representation of the cascade channel $\boldsymbol{H}$ is obtained. This sparse formulation can be further simplified by noticing that the matrix $\boldsymbol{D}$ contains a considerable amount of redundant columns due to the transposed Khatri-Rao product operation. Specifically, we have the following result regarding the redundancy of $\boldsymbol{D}$.

Proposition 1: The matrix $\boldsymbol{D} \in \mathbb{C}^{M \times M_G^2}$ only contains M_G distinct columns which are exactly the first M_G columns of $\boldsymbol{D}$, i.e.

$$\boldsymbol{D}_u = \boldsymbol{D}(:, 1 : M_G) \tag{11}$$

where $\boldsymbol{D}_u$ denotes a matrix constructed by the M_G distinct columns of $\boldsymbol{D}$.

Proof: See Appendix A. ■

Based on this result, the cascade channel $\boldsymbol{H}$ can be further expressed as

$$\boldsymbol{H} = \boldsymbol{D}(\boldsymbol{\alpha}^* \otimes \boldsymbol{\Sigma})\boldsymbol{F}_L^H = \boldsymbol{D}_u\boldsymbol{\Lambda}\boldsymbol{F}_L^H \tag{12}$$

where $\boldsymbol{\Lambda} \in \mathbb{C}^{M_G \times N_G}$ is a merged version of $(\boldsymbol{\alpha}^* \otimes \boldsymbol{\Sigma}) \triangleq \boldsymbol{J}$, with each of its rows being a superposition of a subset of rows in $\boldsymbol{J}$, i.e.

$$\boldsymbol{\Lambda}(i, :) = \sum_{n \in \mathcal{S}_i} \boldsymbol{J}(n, :) \tag{13}$$

where $\boldsymbol{\Lambda}(i, :)$ denotes the ith row of $\boldsymbol{\Lambda}$, $\mathcal{S}_i$ denotes the set of indices associated with those columns in $\boldsymbol{D}$ that are identical to the ith column of $\boldsymbol{D}$. Clearly, there are at most $L \times L'$ nonzero entries in $\boldsymbol{\Lambda}$.

Next, we show how to convert the estimation into a compressed sensing problem by exploiting the sparse structure of the cascade channel. Assuming the pilot signal $s(t) = 1, \forall t$, the received signal $y(t)$ in (2) can be written as

$$\begin{aligned} y(t) =& \boldsymbol{v}^H(t)\boldsymbol{H}\boldsymbol{w}(t)s(t) + \epsilon(t) \\ &\overset{(a)}{=} \left(\boldsymbol{w}^T(t) \otimes \boldsymbol{v}^H(t)\right) \text{vec}(\boldsymbol{H}) + \epsilon(t) \\ &\overset{(b)}{=} \left(\boldsymbol{w}^T(t) \otimes \boldsymbol{v}^H(t)\right) (\boldsymbol{F}_L^* \otimes \boldsymbol{D}_u) \text{vec}(\boldsymbol{\Lambda}) + \epsilon(t) \\ &\overset{(c)}{=} \left(\boldsymbol{w}^T(t) \otimes \boldsymbol{v}^H(t)\right) \tilde{\boldsymbol{F}}\boldsymbol{x} + \epsilon(t) \end{aligned} \tag{14}$$

where (a) and (b) follow from the property of Kronecker product, and in (c) we define

$$\begin{aligned} \tilde{\boldsymbol{F}} &\triangleq \boldsymbol{F}_L^* \otimes \boldsymbol{D}_u \\ \boldsymbol{x} &\triangleq \text{vec}(\boldsymbol{\Lambda}) \end{aligned}$$

Stacking the measurements collected at different time instants $\boldsymbol{y} \triangleq [y(1) \ \ldots \ y(T)]^T$, we arrive at

$$\begin{aligned} \boldsymbol{y} &= \begin{bmatrix} \boldsymbol{w}^T(1) \otimes \boldsymbol{v}^H(1) \\ \vdots \\ \boldsymbol{w}^T(T) \otimes \boldsymbol{v}^H(T) \end{bmatrix} \tilde{\boldsymbol{F}}\boldsymbol{x} + \begin{bmatrix} \epsilon(1) \\ \vdots \\ \epsilon(T) \end{bmatrix} \\ &\triangleq \boldsymbol{\Phi}\boldsymbol{x} + \boldsymbol{\epsilon} \end{aligned} \tag{15}$$

So far we have converted the channel estimation problem into a sparse signal recovery problem, and many classical compressed sensing algorithms such as the orthogonal matching pursuit (OMP) [14] and the basis pursuit (BP) [15] can be employed to estimate the sparse signal $\boldsymbol{x}$. After $\boldsymbol{x}$ is recovered, the cascade channel $\boldsymbol{H}$ can be accordingly obtained via (12).

In the following, we analyze the sample complexity of our proposed compressed sensing-based method. According to the compressed sensing theory, for an underdetermined system of linear equations $\boldsymbol{y} = \boldsymbol{A}\boldsymbol{x}$, the number of measurements required for successful recovery of $\boldsymbol{x}$ is in the order of $k \log n$, where n is the dimension of $\boldsymbol{x}$, and k denotes the number of nonzero elements in $\boldsymbol{x}$. For the sparse signal recovery problem (15), we have $n = M_G N_G$ and $k \leq LL'$. Therefore our proposed method has a sample complexity of $\mathcal{O}(LL' \log(M_G N_G))$. Due to the sparse scattering nature of mmWave channels, LL' is much smaller than MN. Therefore a substantial training overhead reduction can be achieved. Note that the sensing matrix $\boldsymbol{\Phi}$ is a product of two structured matrices. Previous theoretical and empirical studies, e.g. [16], show that structured matrices, especially matrices in a form of Kronecker product, still enjoy nice restricted isometry properties (RIP). Also, we can randomly choose entries of $\boldsymbol{w}(t)$ and $\boldsymbol{v}(t)$ from the unit circle to help obtain a good RIP property.

B. Joint Beamforming Design

Based on the estimated cascade channel $\hat{\boldsymbol{H}}$, we can devise the transmit beamforming vector $\boldsymbol{w}$ and the phase shift matrix $\boldsymbol{\Theta}$ to maximize the received signal power. Such a joint beamforming problem can be cast as

$$\begin{aligned} \max_{\boldsymbol{w}, \boldsymbol{v}} \quad & \left|\boldsymbol{v}^H\hat{\boldsymbol{H}}\boldsymbol{w}\right|^2 \\ \text{s.t.} \quad & \|\boldsymbol{w}\|_2^2 \leq p \\ & \boldsymbol{v} = [e^{j\theta_1} \ \ldots \ e^{j\theta_M}]^H \end{aligned} \tag{16}$$

where p is the maximum transmit power at the BS. Note that for any given $\boldsymbol{v}$, the optimal beamforming vector is $\boldsymbol{w}^\star = \sqrt{p}(\hat{\boldsymbol{H}}^H\boldsymbol{v})/\|\boldsymbol{v}^H\hat{\boldsymbol{H}}\|_2$. Substituting this optimal solution into (16) yields

$$\begin{aligned} \max_{\boldsymbol{v}} \quad & \boldsymbol{v}^H\hat{\boldsymbol{H}}\hat{\boldsymbol{H}}^H\boldsymbol{v} \\ \text{s.t.} \quad & |v_m| = 1 \quad \forall m \end{aligned} \tag{17}$$

where v_m is the mth entry of $\boldsymbol{v}$. The above problem is a non-convex quadratically constrained quadratic program (QCQP), which can be either solved via a semidefinite relaxation (SDR) approach [1] or a manifold optimization approach [17].

V. Simulation Results

In this section, we present simulation results to evaluate the performance of our proposed channel estimation method. In our simulations, three different compressed sensing algorithms, namely, the OMP [14], BPDN [18] and EM-GAMP [19] are employed to solve (15). We assume that the BS employs a uniform linear array (ULA) with $N = 16$ antennas and the IRS is a UPA consisting of $M = 8 \times 8$ passive reflecting elements. In our simulations, we set $N_G = 16$, $M_{G,x} = 10$ and $M_{G,y} = 10$.

To examine the proposed scheme with more practically relevant mmWave channels, we assume a Rician channel comprising a LOS path and a number of NLOS paths [20], [21]. The Rician factor is set to 13.2dB according to [20]. The number of paths for mmWave channels $\boldsymbol{G}$ and $\boldsymbol{h}_r$ are respectively set to $L = 3$ and $L' = 3$, with the AoA and AoD parameters randomly generated. Due to coarse discretization, in our simulations, we do not assume that the true AoA and AoD parameters lie on the discretized grid.

The performance is evaluated via two metrics, i.e. the normalized mean squared error (NMSE) and the average receive signal power ratio (ARSPR). The NMSE is defined as $\mathbb{E}[\|(\hat{\boldsymbol{H}} - \boldsymbol{H})\|_F^2 / \|\boldsymbol{H}\|_F^2]$, where $\hat{\boldsymbol{H}}$ denotes the estimated cascade channel. The ARSPR is defined as the ratio of the actual receive signal power attained based on the estimated channel to the ideal receive signal power, i.e. $\mathbb{E}[\|\boldsymbol{v}^H \boldsymbol{H}\|_F^2 / \|(\boldsymbol{v}^\star)^H \boldsymbol{H}\|_F^2]$, where the phase shift vectors $\boldsymbol{v}$ and $\boldsymbol{v}^\star$ are respectively obtained via solving (17) based on the estimated cascade channel $\hat{\boldsymbol{H}}$ and the real channel $\boldsymbol{H}$. In Fig. 1, we plot the NMSEs and ARSPRs of respective algorithms as a function of the number of measurements T, where the SNR is set to 10dB. From Fig. 1, we see that our proposed method can obtain an accurate channel estimation with only a small number of measurements. For instance, the GAMP only need 110 measurements to reach an NMSE as low as 0.04, thus achieving a substantial overhead reduction for channel estimation. Fig. 2 depicts the NMSEs and ARSPRs versus the SNR, where $T = 100$. We observe that our proposed method can attain an ARPSR close to 1 even in the low SNR regime, which is advantageous for mmWave communications as the SNR before beamforming is usually low.

VI. Conclusions

We studied the problem of channel estimation and joint beamforming design for IRS-assisted mmWave MISO systems. We proposed a compressed sensing-based channel estimation method by exploiting the sparse representation of the cascade channel. Simulation results showed that our proposed method can provide an accurate channel estimation and achieve a substantial training overhead reduction.

Appendix A
Proof of Proposition 1

We partition the matrix $\boldsymbol{D}$ into M_G equal-size blocks, i.e.

$$\boldsymbol{D} = \begin{bmatrix} \boldsymbol{D}_1 & \dots & \boldsymbol{D}_{(u,v)} & \dots & \boldsymbol{D}_{M_G} \end{bmatrix} \tag{18}$$

where $\boldsymbol{D}_{(u,v)} \in \mathbb{C}^{M \times M_G}$ and $(u,v) \triangleq (u-1)M_{G,y} + v$ with $u = 1, \dots, M_{G,x}, v = 1, \dots, M_{G,y}$.

We will prove that $\boldsymbol{D}_{(u,v)} \in \mathbb{C}^{M \times M_G}$ is a column permutation of $\boldsymbol{D}_{(u',v')}$ for any $u' \neq u$ and $v' \neq v$. Specifically, we will show that for any (say, the $(p-1)M_{G,y} + q$)th) column of $\boldsymbol{D}_{u,v}$, which is denoted as $\boldsymbol{D}_{(u,v)}(:, \{p,q\})$, we can always find the same column in $\boldsymbol{D}_{(u',v')}$, where $p = 1, \dots, M_{G,x}$, $q = 1, \dots, M_{G,y}$.

Let the $((m_x - 1)M_y + m_y, (\iota - 1)M_{G,y} + \nu)$th entry of $\boldsymbol{F}_P$ denoted as $\boldsymbol{F}_P(\{m_x, m_y\}, \{\iota, \nu\})$, which is given as

$$\boldsymbol{F}_P(\{m_x, m_y\}, \{\iota, \nu\}) = e^{j2\pi((m_x-1)\theta(\iota) + (m_y-1)\gamma(\nu)} \tag{19}$$

where $\theta(\iota) = -\frac{1}{2} + \frac{\iota - 1}{M_{G,x}}$, $\gamma(\nu) = -\frac{1}{2} + \frac{\nu - 1}{M_{G,y}}$ with $\iota = 1, \dots, M_{G,x}, \nu = 1, \dots, M_{G,y}$, and $m_x = 1, \dots, M_x$, $m_y = 1, \dots, M_y$.

According to the definition of $\boldsymbol{D}$, the $((m_x - 1)M_y + m_y, (p-1)M_{G,y} + q)$th entry of the matrix $\boldsymbol{D}_{(u,v)}$ is given as

$$\begin{aligned} &\boldsymbol{D}_{(u,v)}(\{m_x, m_y\}, \{p,q\}) \\ =&e^{j2\pi\left(\frac{(p-u)(m_x-1)M_{G,y} + (q-v)(m_y-1)M_{G,x}}{M_G}\right)} \end{aligned} \tag{20}$$

Thus we can write $\boldsymbol{D}_{(u,v)}(:, \{p,q\})$ as

$$\begin{aligned} \boldsymbol{D}_{(u,v)}(:, \{p,q\}) = [&\boldsymbol{D}_{(u,v)}(\{1,1\}, \{p,q\}) \\ &\boldsymbol{D}_{(u,v)}(\{1,2\}, \{p,q\}) \ \dots \\ &\boldsymbol{D}_{(u,v)}(\{M_x, M_y\}, \{p,q\})]^T \end{aligned} \tag{21}$$

To find the same column as $\boldsymbol{D}_{(u,v)}(:, \{p,q\})$ in $\boldsymbol{D}_{(u',v')}$, we need

$$\frac{(p'-u')(m_x-1)}{M_{G,x}} + z_p = \frac{(p-u)(m_x-1)}{M_{G,x}} \tag{22}$$

$$\frac{(q'-v')(m_y-1)}{M_{G,y}} + z_q = \frac{(q-v)(m_y-1)}{M_{G,y}} \tag{23}$$

where $z_p, z_q \in \mathbb{Z}$ can be arbitrary integers. Hence, we can arrive at

$$((p'-u') - (p-u))(m_x - 1) = -z_p M_{G,x} \tag{24}$$

$$((q'-v') - (q-v))(m_y - 1) = -z_q M_{G,y} \tag{25}$$

Let $z_p = -z_1(m_x - 1)$ and $z_q = -z_2(m_y - 1)$, $z_1, z_2 \in \mathbb{Z}$, we can find the same column in $\boldsymbol{D}_{(u',v')}$ when p' and q' are set to

$$p' = \text{mod}(p - u + u', M_{G,x}) \tag{26}$$

$$q' = \text{mod}(q - v + v', M_{G,y}) \tag{27}$$

This completes the proof.

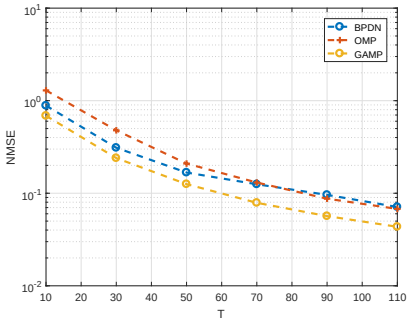

(a) NMSE.

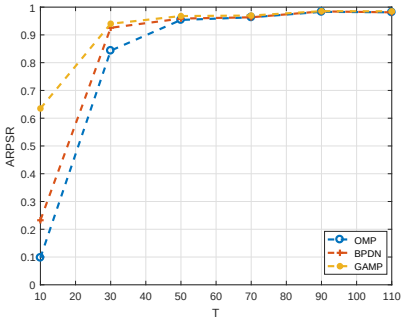

(b) ARSPR.

Fig. 1. NMSEs and ARSPRs of respective algorithms vs. T

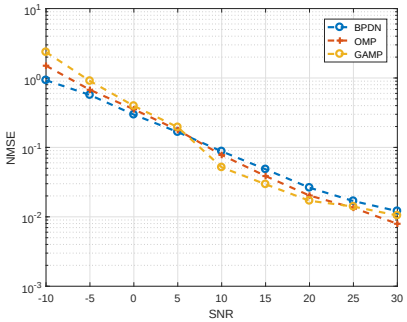

(a) NMSE.

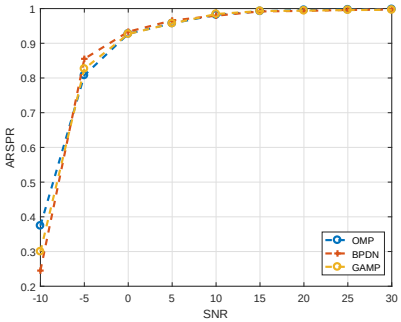

(b) ARSPR.

Fig. 2. NMSEs and ARSPRs of respective algorithms vs. SNR

REFERENCES

[1] Q. Wu and R. Zhang, "Intelligent reflecting surface enhanced wireless network via joint active and passive beamforming," *IEEE Trans. Wireless Commun.*, pp. 1–1, 2019.

[2] E. Basar, M. Di Renzo, J. de Rosny, M. Debbah, M.-S. Alouini, and R. Zhang, "Wireless communications through reconfigurable intelligent surfaces," 2019, [Online]. Available:https://arxiv.org/abs/1906.09490.

[3] X. Tan, Z. Sun, D. Koutsonikolas, and J. M. Jornet, "Enabling indoor mobile millimeter-wave networks based on smart reflect-arrays," in *2018 IEEE Int. Conf. Comput. Commun. (INFOCOM)*, Honolulu, Hawaii, April 15-19, 2018, pp. 270–278.

[4] P. Wang, J. Fang, X. Yuan, Z. Chen, H. Duan, and H. Li, "Intelligent reflecting surface-assisted millimeter wave communications: Joint active and passive precoding design," 2019 [Online]. Available: https://arxiv.org/abs/1908.10734 .

[5] A. Taha, M. Alrabeiah, and A. Alkhateeb, "Enabling large intelligent surfaces with compressive sensing and deep learning." 2019 [Online]. Available: https://arxiv.org/abs/1904.10136 .

[6] D. Mishra and H. Johansson, "Channel estimation and low-complexity beamforming design for passive intelligent surface assisted miso wireless energy transfer," in *2019 IEEE Int. Conf. Acoust., Speech and Signal Process. (ICASSP)*, Brighton,UK, May 12-17 2019, pp. 4659–4663.

[7] T. L. Jensen and E. D. Carvalho, "On optimal channel estimation scheme for intelligent reflecting surfaces based on a minimum variance unbiased estimator," 2019 [Online]. Available: https://arxiv.org/abs/1909.09440.

[8] Z. He and X. Yuan, "Cascaded channel estimation for large intelligent metasurface assisted massive mimo." 2019 [Online]. Available: https://arxiv.org/abs/1905.07948 .

[9] B. Zheng and R. Zhang, "Intelligent reflecting surface-enhanced ofdm: Channel estimation and reflection optimization," 2019 [Online]. Available: https://arxiv.org/abs/1909.03272.

[10] T. S. Rappaport, S. Sun, R. Mayzus, H. Zhao, Y. Azar, K. Wang, G. N. Wong, J. K. Schulz, M. Samimi, and F. Gutierrez, "Millimeter wave mobile communications for 5G cellular: It will work!" *IEEE Access*, vol. 1, pp. 335–349, May 2013.

[11] M. R. Akdeniz, Y. Liu, M. K. Samimi, S. Sun, S. Rangan, T. S. Rappaport, and E. Erkip, "Millimeter wave channel modeling and cellular capacity evaluation," *IEEE J. Sel. Areas Commun.*, vol. 32, no. 6, pp. 1164–1179, June 2014.

[12] A. Alkhateeb, O. E. Ayach, G. Leus, and R. Heath, "Channel estimation and hybrid precoding for millimeter wave cellular systems," *IEEE J. Sel. Topics Signal Process.*, vol. 8, no. 5, pp. 831–846, Oct. 2014.

[13] Y. Ding and B. D. Rao, "Dictionary learning-based sparse channel representation and estimation for fdd massive mimo systems," *IEEE Trans. Wireless Commun.*, vol. 17, no. 8, pp. 5437–5451, 2018.

[14] J. A. Tropp and A. C. Gilbert, "Signal recovery from random measurements via orthogonal matching pursuit," *IEEE Trans. Inform. Theory*, vol. 53, no. 12, pp. 4655–4666, Dec. 2007.

[15] S. S. Chen, D. L. Donoho, and M. A. Saunders, "Atomic decomposition by basis pursuit," *SIAM review*, vol. 43, no. 1, pp. 129–159, 2001.

[16] M. F. Duarte and Y. C. Eldar, "Structured compressed sensing: From theory to applications," *IEEE Trans. Signal Process.*, vol. 59, no. 9, pp. 4053–4085, 2011.

[17] X. Yu, D. Xu, and R. Schober, "MISO wireless communication systems via intelligent reflecting surfaces," 2019, [Online]. Available: https://arxiv.org/abs/1904.12199 .

[18] E. van den Berg and M. P. Friedlander, "SPGL1: A solver for large-scale sparse reconstruction," June 2007, http://www.cs.ubc.ca/labs/scl/spgl1.

[19] J. P. Vila and P. Schniter, "Expectation-maximization gaussian-mixture approximate message passing," *IEEE Trans. Wireless Commun.*, vol. 61, no. 19, pp. 4658–4672, Oct 2013.

[20] S. Hur, T. Kim, D. J. Love, J. V. Krogmeier, T. A. Thomas, and A. Ghosh, "Millimeter wave beamforming for wireless backhaul and access in small cell networks," *IEEE Trans. Commun.*, vol. 61, no. 10, pp. 4391–4403, 2013.

[21] X. Li, J. Fang, H. Duan, Z. Chen, and H. Li, "Fast beam alignment for millimeter wave communications: A sparse encoding and phaseless decoding approach," *IEEE Trans. Signal Process.*, vol. 67, no. 17, pp. 4402–4417, 2019.